12388–12400 *Nucleic Acids Research, 2017, Vol. 45, No. 21* *Published online 23 October 2017*
doi: 10.1093/nar/gkx960

Asialoglycoprotein receptor 1 mediates productive uptake of *N*-acetylgalactosamine-conjugated and unconjugated phosphorothioate antisense oligonucleotides into liver hepatocytes

Michael Tanowitz[1,*], Lisa Hettrick[2], Alexey Revenko[2], Garth A. Kinberger[1], Thazha P. Prakash[1] and Punit P. Seth[1]

[1]Department of Medicinal Chemistry, Ionis Pharmaceuticals, Inc. 2855 Gazelle Court, Carlsbad, CA 92010, USA and [2]Department of Antisense Drug Discovery, Ionis Pharmaceuticals, Inc. 2855 Gazelle Court, Carlsbad, CA 92010, USA

Received April 03, 2017; Revised October 04, 2017; Editorial Decision October 05, 2017; Accepted October 11, 2017

ABSTRACT

Antisense oligonucleotide (ASO) therapeutics show tremendous promise for the treatment of previously intractable human diseases but to exert their effects on cellular RNA processing they must first cross the plasma membrane by endocytosis. The conjugation of ASOs to a receptor ligand can dramatically increase their entry into certain cells and tissues, as demonstrated by the implementation of *N*-acetylgalactosamine (GalNAc)-conjugated ASOs for Asialoglycoprotein Receptor (ASGR)-mediated uptake into liver hepatocytes. We compared the internalization and activity of GalNAc-conjugated ASOs and their parents in endogenous ASGR-expressing cells and were able to recapitulate hepatocyte ASO uptake and activity in cells engineered to heterologously express the receptor. We found that the minor receptor subunit, ASGR2, is not required for effective *in vitro* or *in vivo* uptake of GalNAc-conjugated ASO and that the major subunit, ASGR1, plays a small but significant role in the uptake of unconjugated phosphorothioate ASOs into hepatocytes. Moreover, our data demonstrates there is a large excess capacity of liver ASGR for the effective uptake of GalNAc–ASO conjugates, suggesting broad opportunities to exploit receptors with relatively moderate levels of expression.

The use of short oligonucleotides to alter cellular mRNA levels or pre-mRNA splicing has greatly expanded the breadth of human diseases amenable to drug-based treatment. Oligonucleotides are hydrophilic molecules unable to passively diffuse across lipid bilayers and require chemical modifications and/or nanoparticle complexing to promote cellular internalization via endocytic mechanisms. Antisense oligonucleotides (ASO) containing phosphorothioate (PS) internucleotide linkages, for example, undergo efficient cellular internalization in the absence of transfection reagents or carrier particles (1). This property confers dramatic increases in free ASO potency, both *in vitro* and *in vivo*, through a process that has been termed 'free-uptake' (2).

The identity of cell surface proteins that bind to PS ASOs and the endocytic pathways they mediate comprise a subject of ongoing research and debate (3). It is clear, however, that only a minuscule portion of endocytosed ASO escapes into the cytoplasmic/nuclear space to mediate target cleavage, while the vast majority remains trapped in endocytic compartments and is inactive (4,5). Furthermore, the capacity of cells to functionally internalize ASO to produce target knockdown appears to be independent of the extent to which cells internalize bulk ASO. These observations have led to the hypothesis of separate 'productive' and 'nonproductive' free-uptake pathways, although the molecular mechanisms distinguishing these pathways remain obscure (6). Methods to increase ASO uptake, both generally and into select tissues of interest, hold great therapeutic potential, as would methods to increase the portion of ASO that is directed towards productive cellular uptake.

An emerging strategy that shows great promise entails the conjugation of ASOs to receptor ligands in order to increase ASO potency and distribution to selected tissues (7). For instance, conjugation of triantennary *N*-acetyl galactosamine (GalNAc) to oligonucleotide therapeutics yields 10–30-fold increased potency in isolated hepatocytes, as well as in liver *in vivo* (8–10). There are more than fifteen GalNAc-nucleic acid conjugates in clinical development for

*To whom correspondence should be addressed. Tel: +1 760 603 2433; Email: mtanowitz@ionisph.com

© The Author(s) 2017. Published by Oxford University Press on behalf of Nucleic Acids Research.
This is an Open Access article distributed under the terms of the Creative Commons Attribution License (http://creativecommons.org/licenses/by-nc/4.0/), which permits non-commercial re-use, distribution, and reproduction in any medium, provided the original work is properly cited. For commercial re-use, please contact journals.permissions@oup.com

a variety of disease indications and clinical data demonstrate the effectiveness of this approach. GalNAc conjugation confers high affinity binding to the Asialoglycoprotein Receptor (ASGR), a cell surface C-type lectin that functions as a scavenger receptor and is able to remove desialylated glycoproteins from circulation (11–13). The ASGR is a highly expressed, high capacity endocytic receptor in hepatocytes and its successful implementation as an ASO-conjugate carrier may largely be due to its ability to substantially increase bulk ASO uptake into liver. As a natural ligand/receptor system, however, the GalNAc/ASGR interaction may also more efficiently sort ASOs towards a productive cellular pathway compared to the poorly defined binding and internalization pathways utilized by unconjugated phosphorothioate oligonucleotides.

We sought to explore the relationship between ASO uptake and the increased potency conferred by GalNAc conjugation by directly comparing ASO potency to the kinetics and extent of ASO internalization in hepatic cell lines and primary cells representing varying levels of ASGR expression. Using flow cytometry we were able to compare the maximal uptake rates (V_{max}) and concentrations producing half maximal uptake (endocytic K_m) of parent and GalNAc3-conjugated ASOs, and by applying an excess of free GalNAc we were able to isolate and measure the ASGR-mediated component of conjugate internalization. Surprisingly, we found that a relatively small portion of ASO internalized via the ASGR mediated a >10-fold increase in potency in murine primary hepatocytes. Interestingly, despite displaying a more significant portion of ASGR-mediated uptake of ASO conjugate compared to murine primary hepatocytes, HepG2 human hepatoma cells showed no significant potency differences between parent and GalNAc-conjugated ASO.

To understand the relative importance of the two ASGR sub-units in ASO uptake, we created stably transfected human embryonic kidney (HEK) cell lines expressing the human ASGR1 and ASGR2 individually or concurrently. When stably expressed in HEK 293 cells, ASGR1 conferred a 3–4-fold increase in uptake of the ASO conjugate corresponding to as much as a 50-fold increase in knockdown potency. Surprisingly, co-expression of ASGR2 was without apparent effect, and appeared to be dispensable for functional uptake of GalNAc ASOs. We also uncovered evidence that the ASGR is capable of contributing to uptake of unconjugated PS ASOs, in addition to its well- established role in uptake of GalNAc ASO conjugates. Importantly, we confirmed that the results from HEK 293 cells are relevant in animals by characterizing the relationship between ASGR1 and ASGR2 reduction in mouse liver and the resulting effects on GalNAc and unconjugated PS ASO potency in the liver. Our results indicate there is a large excess capacity of ASGR-mediated ASO uptake activity *in vivo*, suggesting a wide opportunity to target receptors with expression levels that are low relative to liver ASGR.

MATERIALS AND METHODS

Synthesis of ASOs

The synthesis of ASOs were achieved as reported previously (9). The ASOs were synthesized at 2–40 μmol scale using UnyLinkerTM support functionalized by modified nucleoside or GalNAc cluster. A 0.1 M solution of Cy3-phosphoramidite (Glen Research, 22825 Davis Drive, Sterling, Virginia, USA) was used for incorporation of Cy3- dye at 5′-end of ASO. For the synthesis of ASOs, 0.1 M solutions of all phosphoramidites in acetonitrile, and standard oxidizing and capping reagents were used. For each ASO structure 4–9-fold excess of phosphoramidite was delivered with a 8-min coupling time. The 5′-end dimethoxytrityl or monomethoxytrityl group was left on to facilitate purification. To remove cyanoethyl protecting groups from the phosphorothioate (PS) or phosphodiester (PO) linkages, all ASOs were treated post-synthetically with 1:1 triethylamine: acetonitrile. Cy3- containing ASOs were treated with aqueous NH4OH for 24 h at room temperature and all other ASOs were heated with aqueous NH_4OH at 55°C for 9–12 h to cleave from support, remove protecting groups, and hydrolyze the UnyLinkerTM moiety. ASOs were purified by ion-exchange chromatography using a gradient of NaBr across a column packed with Source 30Q resin. Final 5′-end dimethoxytrityl or monomethoxytrityl group was removed on ion-exchange column using 0.8% dichloroacetic acid in water. Pure fractions were desalted using high performance liquid chromatography (HPLC) on a reverse phase column. Purity and mass of ASOs were determined using ion-pair liquid chromatography mass spectrometry (LCMS) analysis (Supplementary Table S1).

Cell culture

Huh-7, Hek293 and HepG2 cells were grown according to the protocols provided by the American Type Culture Collection (ATCC, Manassas, VA, USA). Cells were seeded at 50% confluency, incubated for 16 hrs, and then ASO uptake, ASO activity or immunofluorescence analysis was performed.

Primary murine hepatocyte isolation

Mouse liver was perfused as previously described (14,15). Briefly, mice were anesthetized with an intraperitoneal injection of 0.1 ml per 10 g ketamine/xylazine. Inferior vena cava was catheterized and clamped. Liver was perfused with Hank's Balanced Salt Solution (Life Technologies) and mesenteric vessel was cut for drainage. Liver was subsequently perfused with collagenase (Roche). Following the perfusion, liver was removed and gently messaged through sterile nylon mesh. Cells were washed in Williams E (Life Technologies) containing 10% fetal calf serum, (4-(2-hydroxyethyl)-1-piperazineethanesulfonic acid) (HEPES), L-glutamine and antibiotic/antimycotic. *Cell separations:* Liver perfusions were performed as described above. A portion of the whole liver cell suspension was collected for the whole liver fraction. The fraction was spun at 450 × g, washed with PBS containing 0.5% BSA and 2 mM EDTA (wash buffer), and pelleted. The hepatocyte and np fractions were separated as described previously. (16). Whole liver cell suspension was spun at 50 × g. The resulting hepatocyte pellet was washed, spun and run over a 30% percoll (GE Healthcare) gradient. A final wash was performed to remove residual percoll and cells were subsequently pelleted.

Animals and oligonucleotide dosing

Seven-week-old male BALB/c mice (Charles River Laboratories) were treated according to the indicated schedules. The animals were housed in micro-isolator cages on a constant 12 h light–dark cycle with controlled temperature and humidity and were given access to food and water *ad libitum*. All animal husbandry and procedures performed at Ionis Pharmaceuticals (CA, USA) were approved by the Institutional Animal Care and Use Committee.

All antisense oligonucleotides were administered subcutaneously as a sterile-filtered phosphate buffered saline (PBS) solution at a concentration which allows delivering of a specified weekly dose in two injections, each 1/100th of the body volume.

Typical experiment consisted of 3-week treatment period with mouse Asgr ASOs (depletion of ASGR proteins) followed by single injection of mouse fXI 'parent' or THA-GN3 conjugated ASO. Animals were sacrificed 48 h after fXI ASO treatment for gene expression analysis in the liver.

For gene expression analysis mouse liver samples were homogenized in RLT buffer (Qiagen) containing 1% 2-mercaptoethanol. Total mRNA was prepared using PureLink™ Total RNA Purification Kit (Life Technologies). The amount of specific mRNA was analyzed using a StepOne™ Real-Time PCR System (Life Technologies). Primer and probe sequences were as follows: mouse Asgr1 (forward – GCACCTGGACAATGATAATGAC, reverse – GATC ACACAGACAACCACCA, probe – CTCTCCTCGAGC CTCAGCATTCTG), mouse Asgr2 (forward – CTACTG GTTTTCTCGGGATGG, reverse – CAAATATGAAAC TGGCTCCTGTG, probe – ACAACAAAGTCCTGCT CCTCCCTG), mouse fXI (forward – ACATGACAGGCG CGATCTCT, reverse – TCTAGGTTCACGTACACATC TTTGC, probe – TTCCTTCAAGCAATGCCCTCAGCA ATX) and mouse glyceraldehyde-3-phosphate dehydrogenase (*Gapdh3*) (forward – TGTGTCCGTCGTGGATCT GA, reverse – CCTGCTTCACCACCTTCTTGA, probe – CCGCCTGGAGAAACCTGCCAAGTATG). Expression levels of particular mRNA were normalized to Gapdh3 mRNA levels and expressed as % from the average of PBS group.

Free uptake, RNA preparation and qRT-PCR

One day prior to free uptake assays cells were seeded into 96-well plates (∼10,000 cells per well) and allowed to attach for at least 16 hours. ASOs were diluted into complete growth over a 12-point 3-fold dilution series at 10× final concentration. Diluted ASOs were then applied to triplicate treatment wells at 0.1× final volume and plates were returned to the incubator for 20–24. Total RNA was prepared using an RNeasy mini kit (Qiagen, Valencia, CA, USA) from cells grown in 96-well plates. qRT-PCR was performed using TaqMan primer probe sets. Briefly, ∼50 ng total RNA in 5 μl water was mixed with 0.3 μl primer probe sets containing forward and reverse primers (10 μM of each) and fluorescently labeled probe (3 μM), 0.3 μl RT enzyme mix (Qiagen), 4.4 μl RNase-free water, and 10 μl of 2 × PCR reaction buffer in a 20 μl reaction. Reverse transcription was performed at 48°C for 10 min, 40 cycles of PCR were conducted at 94°C for 20 s, and 60°C for 20 s within each cycle, using StepOne Plus RT-PCR system (Applied Biosystems, Phoenix, AZ, USA). The mRNA levels were normalized to the amount of total RNA present in each reaction as determined for duplicate RNA samples by Ribogreen assay (Life Technologies).

Immunofluorescence staining

Cells were fixed with 4% paraformaldehyde for 30 min at room temperature and were permeabilized with 0.05% saponin (Sigma) in PBS for 5 min. Cells were treated with blocking buffer (1 mg/ml BSA in PBS) for 30 min and then incubated with primary antibodies (1:100–1:200 in blocking buffer) at room temperature for 2 h. Following three washes with PBS, cells were incubated with fluorescently labeled secondary antibodies (1:200 in blocking buffer) at room temperature for 1 hr. After washing, slides were mounted with Prolong Gold anti-fade reagent with DAPI (Life Technologies) and imaged using a confocal microscope (Olympus FV-1000).

Protein isolation and western blotting

Cells were lysed, and samples were incubated at 4°C for 30 min in RIPA buffer (50 mM Tris–HCl, pH 7.4, 1% Triton X-100, 150 mM NaCl, 0.5% sodium deoxycholate, and 0.5 mM EDTA). Proteins were separated by SDS-PAGE using 4–20% Novex Tris-Glycine gradient Gels (Life Technologies) and electroblotted onto nitrocellulose membranes using the iBLOT2 transfer system (Life Technologies). The membranes were blocked with 5% non-fat dry milk in TBS/0.1% Tween-20 at 4°C overnight. Membranes were then incubated with primary antibodies at room temperature for 1 h. After three washes with TBS-T, the membranes were incubated with appropriate HRP-conjugated secondary antibodies (1:5000) at room temperature for 1 h prior to image development using ECL reagents (Abcam, Cambridge, MA, USA).

Measurement of ASO uptake by flow cytometry

For flow cytometry experiments cells were seeded in 24-well plates (∼150 000 cells/well) and allowed to attach and equilibrate for at least 16 h. The indicated Cy3-lableled ASOs were added to wells over a 6-point 3-fold dilution series and incubated for two hours. Two plates were prepared for each treatment condition, one serving as 4°C no internalization control that was kept on ice during incubation, while the second plate was incubated at 37°C to allow for energy-dependent internalization. Following the incubation period all plates were placed on ice and washed three times with ice-cold PBS/3% BSA/2 mM EDTA then lifted with trypsin, diluted into wash buffer, and placed into flow cytometry tubes on ice. Cells then analyzed by flow cytometry for mean fluorescence intensity using a BD FACSCalibur flow cytometer (BD Biosciences, San Jose, CA, USA). Internalized ASO was expressed as the difference between the corresponding 4°C and 37°C mean fluorescence intensities.

Generation of ASGR expressing cell lines

HEK cells stably expressing hASGR1 or hASGR2 were generated by transient transfection of pcDNA3.1 Hygro

(+)—ASGR1 or pcDNA 3.1 Hygro (+)—ASGR2 followed by long term selection with hygromycin. Colonies obtained by limiting dilution were assayed for receptor expression and uptake activity prior to further manipulation. HEK cells stably expressing both hASGR1 and hASGR2 were generated by infecting ASGR2 clone 2A3 with ASGR1 lentivirus produced by transfection of 293T cells with pLVX-IRES-Puro (Clontech Laboratories Inc., Mountainview, CA) harboring the ASGR1 insert. Infected cells were selected with hygromycin/puromycin and then analyzed for receptor expression by western blot and immunofluorescence. HEK cells engineered for inducible ASGR1 expression were generated via transfection of pcDNA 5/FRT/TO – ASGR1 into the FLP-In T-Rex 293 cell line (ThermoFisher Scientific, Waltham, MA) followed by selection with hygromycin.

RESULTS

The Asialogylcoprotein Receptor (ASGR) is primarily expressed in hepatocytes where it regulates the serum concentration of endogenous 2,6-linked sialoglycoproteins and mediates clearance of exogenously applied asialoglycoproteins (12,17). Previous work by Lee et al elegantly demonstrated that tri-antennary n-acetylgalactosamine (GalNAc) is a high affinity ligand for ASGR (18). To compare ASGR-mediated uptake and potency of GalNac-modified ASOs we utilized three hepatic cell culture models (Huh7 and HepG2 human hepatocarcinoma cell lines, and primary murine hepatocytes) representing low, medium, and high expression of ASGR receptors (Supplementary Figure S2). In order to measure ASO internalization with sensitivity and precision we utilized a flow cytometric assay employing Cy3-labeled ASOs (19).

Phosphorothioate backbone modifications confer both nuclease stability and protein binding properties to ASOs. In contrast to phosphodiester-based ASOs, phosphorothioate ASOs are robustly internalized into cells in the absence of transfection reagents or ligand-conjugation (1). To isolate the ASGR-mediated component of ASO internalization by flow cytometry we employed two complementary strategies (Supplementary Figure S1, Figure 1A and B): (i) we examined the uptake of both full 2′-*O*-(2-methoxyethyl)-RNA (MOE) (20) phosphodiester and phosphorothioate 5–10-5 MOE gapmer ASOs grouped into parent and GalNAc-conjugated pairs and (ii) uptake of these ASOs was further examined with and without an excess of competing free GalNAc ligand. As MOE-RNA is nuclease-resistant, a uniform MOE chemistry was chosen for the PO ASOs to eliminate the possibility of media-borne nuclease activity confounding the uptake results. Such ASOs do not activate RNAse H as they lack the DNA 'gap' region responsible for RNAse H recognition of RNA/DNA heteroduplexes.

Uptake of GalNAc ASOs in hepatoma cell line with low/null ASGR expression

In the ASGR-low/null cell line Huh-7, the GalNAc-conjugate had lower uptake than the unmodified parent (Figure 1A). This effect is unrelated to ASGR expression as excess free GalNAc3 was without effect. Uptake of the uniform MOE phosphodiester versions of these ASOs were then examined in a similar fashion. As expected, uptake of parent phosphodiester ASO was far less than the PS counterpart and the estimated Km exceeded the concentrations tested (Figure 1B). Once again, uptake of the corresponding GalNAc-conjugated version was lower than the parent. Lower uptake of ligand-conjugated ASOs in receptor negative cells appears to be a common phenomenon (Figure 1A, B and data not shown) and is likely to be a non-specific effect due to interference with optimal phosphorothioate binding. An excess of competing free GalNAc ligand again had no effect on ASO uptake. The activity of the corresponding unlabeled phosphorothiorate 5–10–5 MOE gapmer ASOs, as measured by MALAT-1 mRNA reduction, was also determined in Huh-7 (Figure 1C). In agreement with the uptake data, the GalNAc conjugate produced lower activity than the unmodified parent.

Uptake of GalNAc ASOs in hepatoma cell line with robust ASGR expression

We next examined uptake in HepG2 cells which are reported to have 50 000–75 000 copies/cell of ASGR (21). In contrast to the results from Huh-7 cells, the ASGR positive HepG2 cells showed ∼50% increased uptake of GalNAc-conjugated PS ASO (Figure 1A). Furthermore, the increase in uptake was reduced when excess free GalNAc was applied. Surprisingly, excess free GalNAc reproducibly increased uptake of the unconjugated parent ASO, the precise mechanism of which is not clear at present. Uptake of the phosphodiester ASOs in HepG2 cells produced much more dramatic results (Figure 1B). Very little of the parent PO ASO was internalized, whereas a relatively large amount of uptake was observed for the GalNAc-conjugate. As expected, uptake of the PO conjugate was nearly eliminated by competing free GalNAc ligand. Interestingly, the Km for uptake of the PO conjugate was large relative to the Kd of the GalNAc3-ASGR interaction (10–20 nM, 9) and was, in fact, significantly higher than the Km of the parent or GalNac conjugated PS ASOs. Unfortunately, HepG2 cells show exceedingly poor free uptake activity despite their significant internalization of bulk ASO, yielding an IC_{50} approximating the highest dose tested, 100 μM. Nevertheless, there was no evidence of improved knockdown activity for the GalNAc-conjugate compared to the parent ASO (Figure 1C).

Uptake of GalNAc ASOs in fresh primary mouse hepatocytes

The uptake of GalNAc ASOs in freshly isolated primary mouse hepatocytes, which retain ASGR expression (22), was also investigated. In contrast to the human hepatoma cell lines, primary murine hepatocytes represent a cell culture model that has consistently been shown to recapitulate the increased potency of GalNAc–ASO conjugates observed *in vivo.* Increased uptake of the GalNAc conjugated phosphorothioate ASO, however, was surprisingly modest in primary murine hepatocytes and was less than that observed for HepG2 cells (Figure 1A). This modest increase in conjugate uptake was nonetheless eliminated by excess free ligand, demonstrating its specificity. Similar to HepG2 cells,

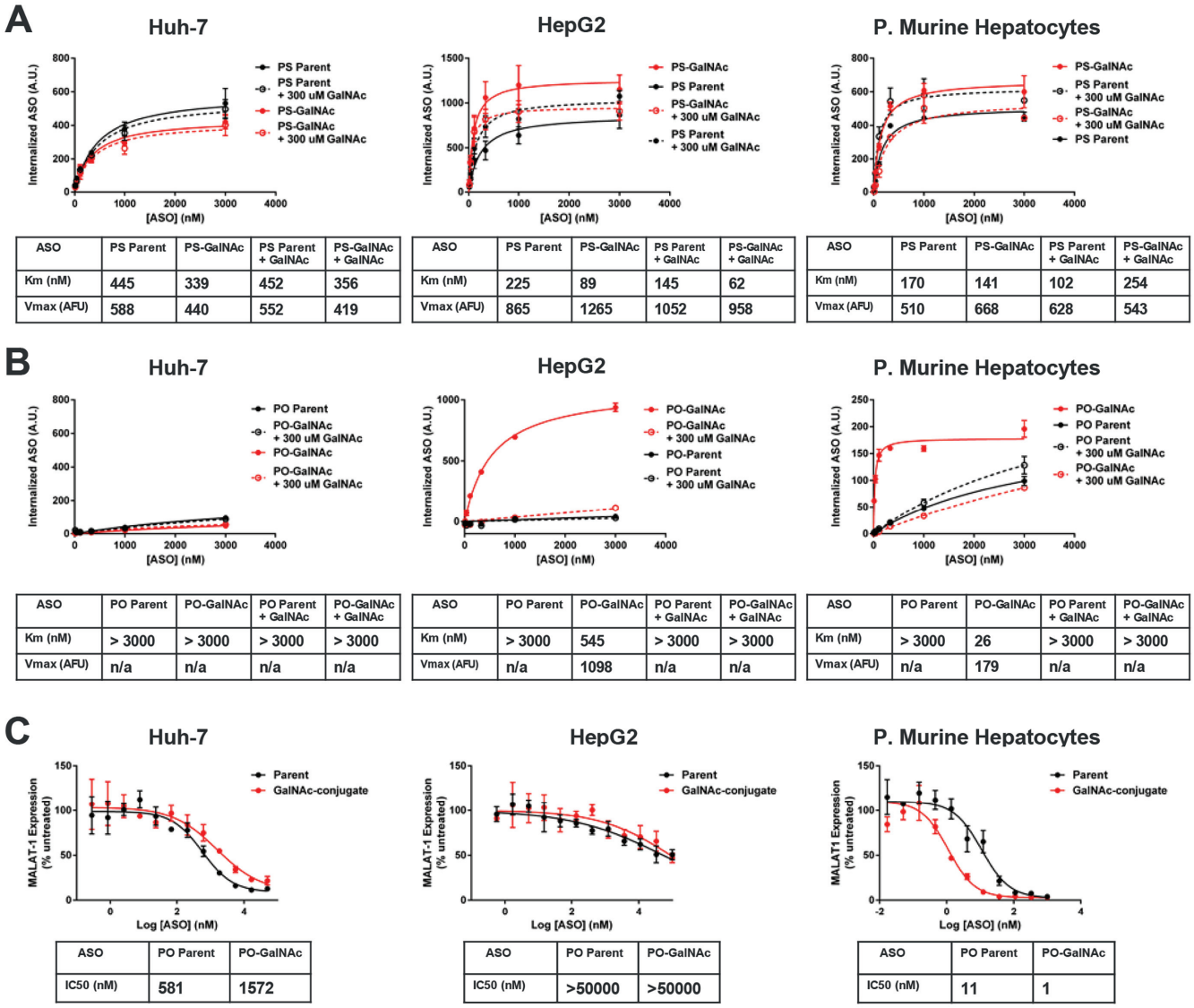

ASO	PS Parent	PS-GalNAc	PS Parent + GalNAc	PS-GalNAc + GalNAc
Km (nM)	445	339	452	356
Vmax (AFU)	588	440	552	419

ASO	PS Parent	PS-GalNAc	PS Parent + GalNAc	PS-GalNAc + GalNAc
Km (nM)	225	89	145	62
Vmax (AFU)	865	1265	1052	958

ASO	PS Parent	PS-GalNAc	PS Parent + GalNAc	PS-GalNAc + GalNAc
Km (nM)	170	141	102	254
Vmax (AFU)	510	668	628	543

ASO	PO Parent	PO-GalNAc	PO Parent + GalNAc	PO-GalNAc + GalNAc
Km (nM)	> 3000	> 3000	> 3000	> 3000
Vmax (AFU)	n/a	n/a	n/a	n/a

ASO	PO Parent	PO-GalNAc	PO Parent + GalNAc	PO-GalNAc + GalNAc
Km (nM)	> 3000	545	> 3000	> 3000
Vmax (AFU)	n/a	1098	n/a	n/a

ASO	PO Parent	PO-GalNAc	PO Parent + GalNAc	PO-GalNAc + GalNAc
Km (nM)	> 3000	26	> 3000	> 3000
Vmax (AFU)	n/a	179	n/a	n/a

ASO	PO Parent	PO-GalNAc
IC50 (nM)	581	1572

ASO	PO Parent	PO-GalNAc
IC50 (nM)	>50000	>50000

ASO	PO Parent	PO-GalNAc
IC50 (nM)	11	1

Figure 1. Uptake and activity of parent and GalNAc-conjugated ASOs. (**A**) Uptake of parent and GalNAc-conjugated phosphorothioate ASOs in three hepatocyte cell culture models. Increased uptake of the GalNAc ASO conjugate and competition by free GalNAc is observed in ASGR-expressing cells, HepG2 and primary murine hepatocytes, but not the ASGR null cell line Huh-7. (**B**) Uptake of parent and GalNAc-conjugated phosphodiester ASOs in three hepatocyte cell culture models. Uptake of the GalNAc ASO conjugate and competition by free GalNAc is observed in ASGR-expressing cells, HepG2 and primary murine hepatocytes, but not the ASGR null cell line Huh-7. (**C**) Knockdown activity parent and GalNAc-conjugated phosphorothioate ASOs in three hepatocyte cell culture models. Increased potency of the GalNAc–ASO conjugate is observed only in primary murine hepatocytes.

excess free ligand resulted in a small but consistent increase in uptake of the unconjugated parent ASO, suggesting this effect depends upon ASGR expression.

As in HepG2 cells, the full MOE phosphodiester ASOs produced the most striking differentiation between parent and ASO conjugate (Figure 1B). The phosphodiester GalNAc-conjugate displayed much higher uptake than the phosphodiester parent and this increased uptake was eliminated by excess free ligand. In contrast to the results obtained in HepG2 cells, the endocytic Km for the PO conjugate was much lower than the parental PS sequence and approached the K_d value of the ASGR/GalNAc–ASO interaction (9). Primary murine hepatocytes from the same isolates were tested in parallel for IC50 determination. In agreement with previous reports (23), we observed a 10-fold increase in ASO potency for the GalNAc-conjugated ASO (Figure 1C).

Generation of HEK-ASGR stable cell line

The conflicting results obtained for the relationship between uptake and potency shifts in HepG2 cells versus primary hepatocytes were surprising and highlighted the complications involved in comparing cells of different origins possessing different intrinsic sensitivities to ASO-mediated knockdown. To directly compare ASO uptake and potencies conferred by ASGR expression we generated HEK 293 cells stably expressing active ASGR. With this approach we were able to study ASGR-mediated gains in ASO uptake

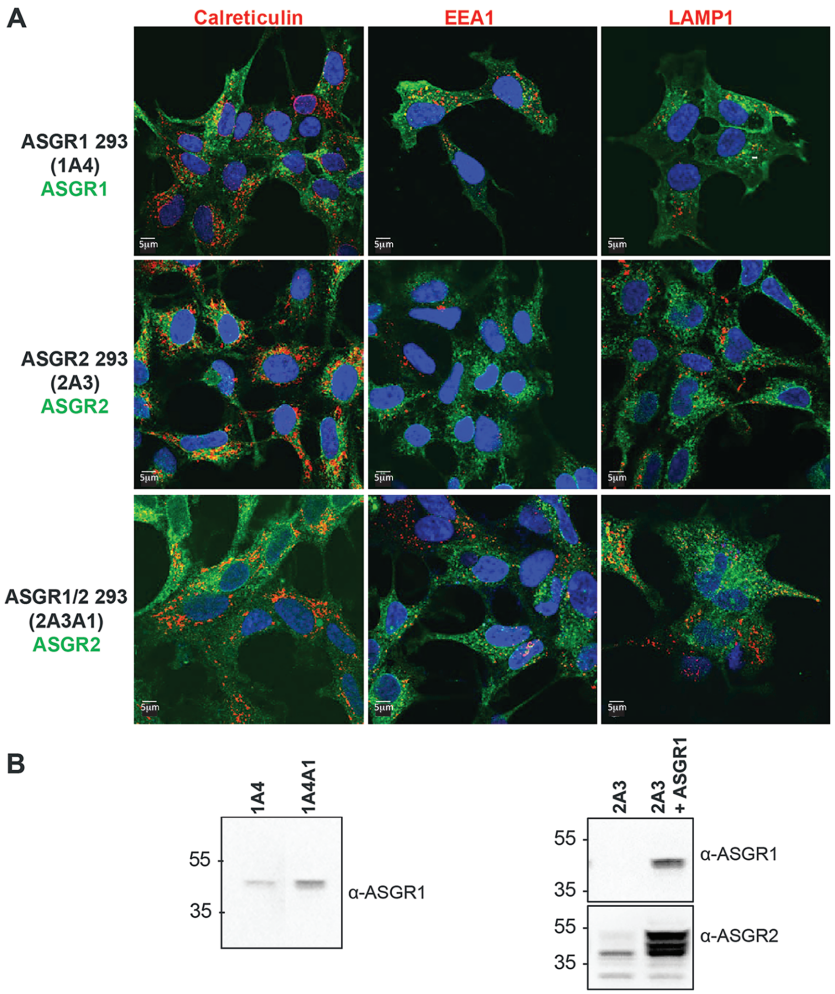

Figure 2. Generation of ASGR-expressing HEK 293 cell lines (**A**) Immunofluorescence images from cells stably expressing ASGR1 and/or ASGR2. ASGRs are labeled in green, compartment markers are labeled in red. Co-expression with ASGR1 results in plasma membrane localization of ASGR2. (**B**) Western blots from cells stably expressing ASGR1 and/or ASGR2. Cell line 2A3 stably expressing ASGR2 was infected with ASGR1 lenti-virus to produce the ASGR1/ASGR2 double stable cell line 2A3A1. For comparison, cell line 1A4 stably expressing ASGR1 was infected with ASGR1 lenti-virus to produce the higher expressing line 1A4A1.

and potency against an isogenic cellular background. The ASGR is composed of both a major (ASGR1) and minor subunit (ASGR2) (24). ASGR1 has been shown to be efficiently targeted to the plasma membrane and to undergo constitutive endocytosis and recycling (25).

In agreement, we observed ASGR1 to display a distribution split between the plasma membrane and endomembrane compartments representing ASGR1 in the endocytic pathway, as evidenced by a lack of colocalization with calreticulin, an ER marker, and partial colocalization with the early endosome marker EEA1 (Figure 2A, top panels). Furthermore, western blot of cells stably expressing ASGR1 produced a single band migrating at ∼45 kDa, consistent with the mature glycosylated, post-Golgi species (25) (Figure 2B, left panel). ASGR2 lacks the ER export signal present in ASGR1 and has been reported to be largely retained in the ER and rapidly degraded (26). Consistent with this, we detected no evidence ASGR2 was delivered to the plasma membrane; rather, we observed endomembrane staining that substantially colocalized with calreticulin (Figure 2A, middle panels). Western blot of these cells revealed a predominate ASGR2 species migrating at ∼40 kDa, representing immature ASGR2, with minor diffuse higher molecular weight bands likely to be ASGR2 that escaped the ER and underwent mature glycosylation (26) (Figure 2B). Strikingly, ASGR2 cells infected with ASGR1 virus revealed an overall higher ASGR2 immunofluorescence with the appearance of ASGR2 at the plasma membrane, partial colocalization with EEA1, and residual colocalization with Calreticulin (Figure 2A, bottom panels). Moreover, co-expression of ASGR1 resulted in the appearance of dominant higher migrating ASGR2 immunoreactive bands on western blots that are consistent with post-ER glycosylation (Figure 2B). This data parallels previous reports demonstrating that co-expression of ASGR1 results in ASGR2 incorporation into ASGR1/ASGR2 heterodimers that are then exported from the ER and are ultimately targeted to the plasma membrane (25).

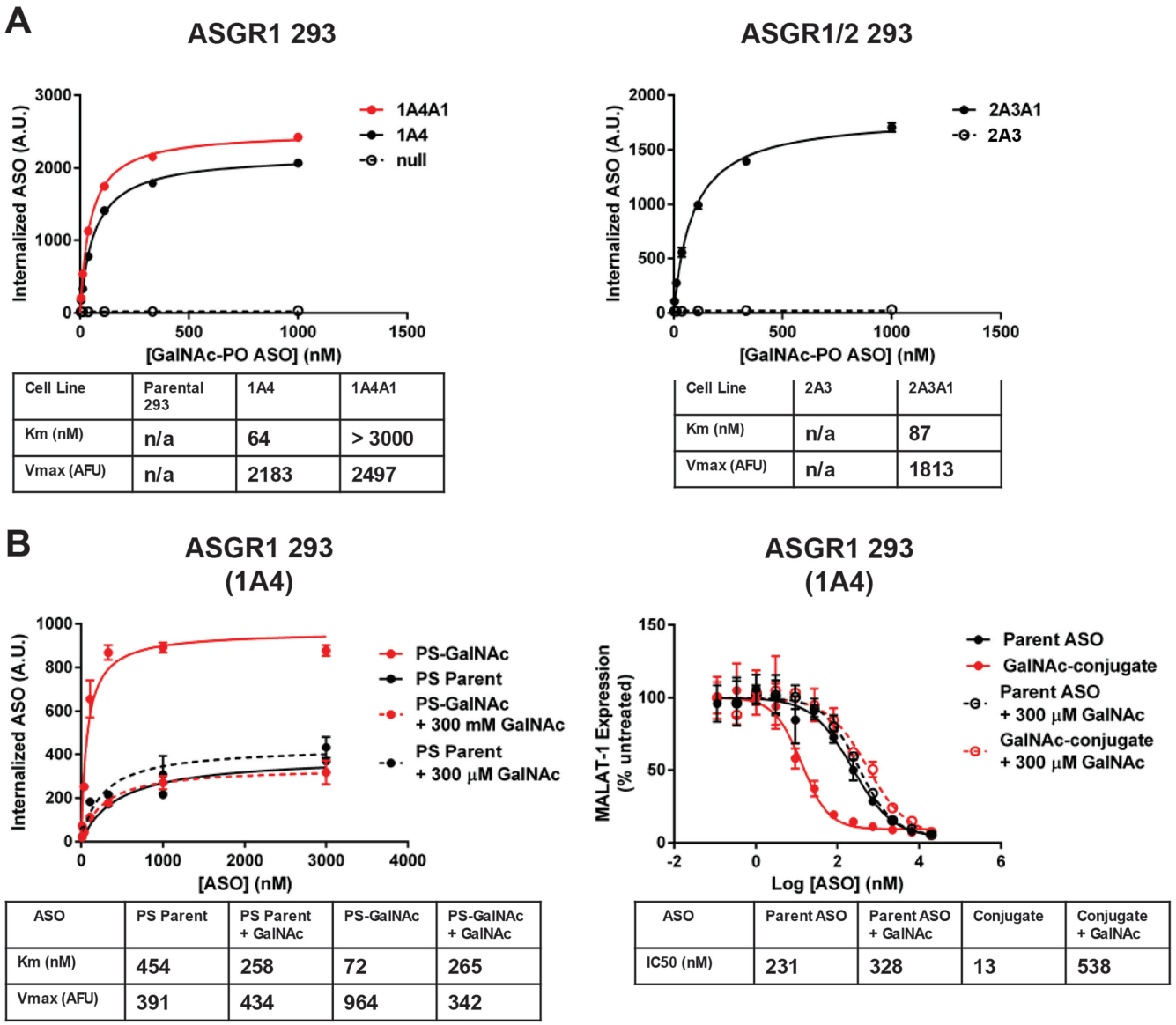

Cell Line	Parental 293	1A4	1A4A1
Km (nM)	n/a	64	> 3000
Vmax (AFU)	n/a	2183	2497

Cell Line	2A3	2A3A1
Km (nM)	n/a	87
Vmax (AFU)	n/a	1813

ASO	PS Parent	PS Parent + GalNAc	PS-GalNAc	PS-GalNAc + GalNAc
Km (nM)	454	258	72	265
Vmax (AFU)	391	434	964	342

ASO	Parent ASO	Parent ASO + GalNAc	Conjugate	Conjugate + GalNAc
IC50 (nM)	231	328	13	538

Figure 3. Expression of ASGR1 is sufficient to mediate increased uptake and activity GalNAC-ASO conjugates in HEK 293 cells. (**A**) Uptake of parent and GalNAC-conjugated phosphodiester ASOs in HEK 293 cells expressing ASGR1 and/or ASGR2. (**B**) Uptake and activity of parent and GalNAc-conjugated phosphorothioate ASOs in ASGR1-expressing clone 1A4. GalNAc conjugation produces and 18-fold shift in IC_{50} that is eliminated by competing free GalNAc.

ASGR2 is not required for uptake of GalNAc ASOs in ASGR HEK-293 cells

To isolate ASGR-mediated internalization, we next analyzed uptake of the phosphodiester ASO GalNAc conjugate in the engineered cell lines and observed robust uptake only in ASGR1-expressing clones (Figure 3A). Interestingly, the parameters of conjugate uptake in cells expressing only ASGR1 were similar to those from cells expressing both ASGR1 and ASGR2, suggesting ASGR1 homooligomers are sufficient for GalNAc-mediated ASO uptake. Of particular note, we observed a low Km of uptake similar to that seen with primary murine hepatocytes. When uptake of phosphorothioate containing ASOs were measured in the ASGR1-expressing cells the results recapitulated those seen in both HepG2 and primary hepatocytes: there was a pronounced increase in uptake of the GalNAc-conjugate relative to the parent ASO that was eliminated by free GalNAc, while uptake of the parent ASO was slightly increased by excess free GalNAc (Figure 3B). When this line was tested in free uptake activity assays the GalNAc conjugate was 18-fold more potent than the parent ASO and this improvement was likewise eliminated by excess free GalNAc (Figure 3B). When activity of the GalNAc–ASO conjugate was tested in the ASGR1/ASGR2 co-expressing cell line we found no discernable difference from the line expressing ASGR1 alone (Figure 4A).

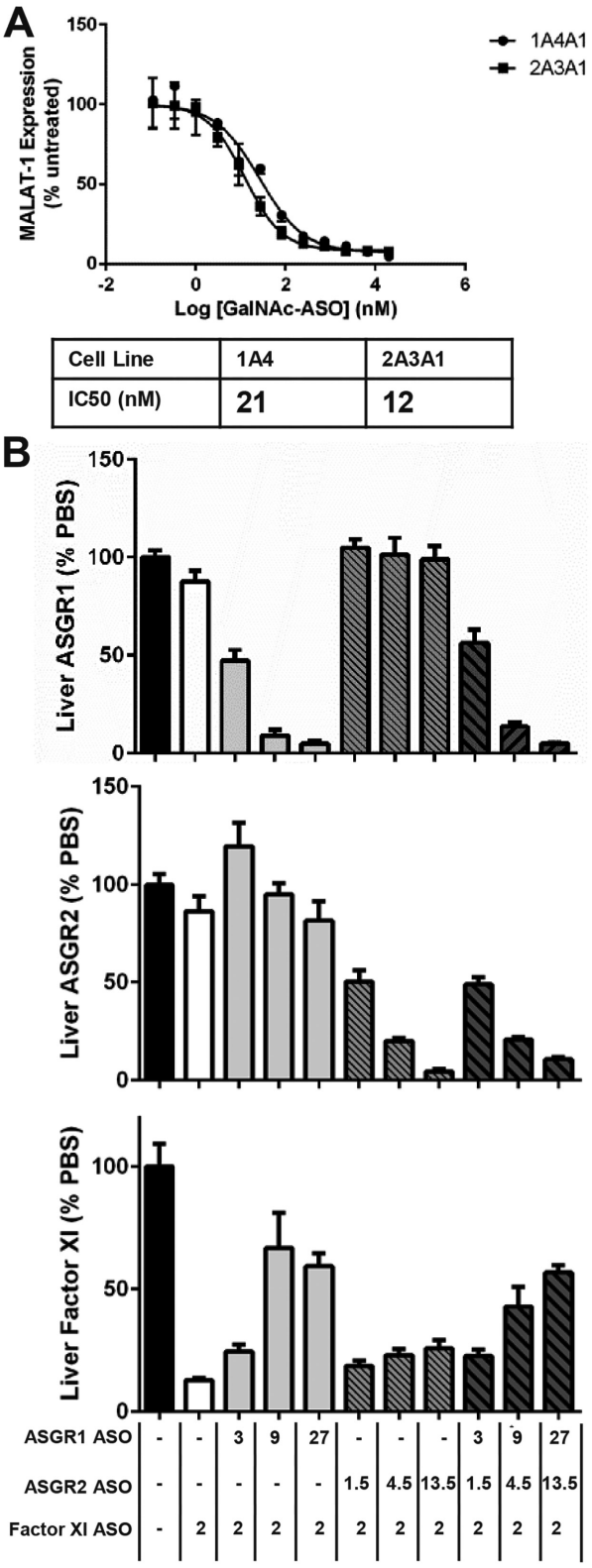

Figure 4. ASGR2 is not required for increased potency of GalNAc-conjugated ASOs *in vitro* or *in vivo*. (**A**) Dose-response and IC50 of GalNAc–ASO conjugate in ASGR1 vs ASGR1/ASGR2 receptor expressing HEK 293 cells. (**B**) Activity of GalNAc-conjugated ASO dosed alone or in combination with ASOs targeting ASGR1 and/or ASGR2 in mouse liver. Doses are expressed as mg ASO/kg body weight.

ASGR2 is not required for uptake of GalNAc ASOs in the liver

Taken together, the above results suggested that the ASGR1 expressing HEK cells reproduced the patterns of uptake and activity seen in primary murine hepatocytes, and suggested that ASGR2 is dispensable for uptake of GalNAc–ASO conjugates. To test this hypothesis *in vivo*, mice were pretreated with ASOs targeting ASGR1 and/or ASGR2 to deplete liver of the respective subunits, followed by treatment with a GalNAc–ASO conjugate targeting Factor XI (9). Knockdown of ASGR1 dose-dependently reduced the activity of the Factor XI GalNAc–ASO conjugate, whereas knockdown of ASGR2 had little to no effect (Figure 4B). This result would appear to conflict with reports that ASGR2 is required for high affinity binding and uptake of a model asialoglycoprotein, asialoorsomucoid (27). In agreement with our results, however, it has previously been shown that ASGR2 is dispensable for *in vivo* uptake of a different asialoglycoprotein receptor substrate, vWF (28). Given the apparent irrelevance of ASGR2 for uptake of GalNAc–ASO conjugates, all further work was conducted with lines expressing only ASGR1.

Role of backbone chemistry and 2′-modifications on activity of GalNAc ASOs in ASGR HEK cells

Given the importance of phosphorothioate content in uptake of unconjugated ASOs we were interested in testing the role played by backbone chemistry in uptake of GalNAc–ASO conjugates, as such uptake represents a combination of receptor-targeted and phosphorothioate-mediated uptake. We therefore examined uptake of ASOs possessing different phosphorothioate content: full PS containing 5–10–5 MOE and a mixed backbone version with phosphodiester replacing six phosphorothioate nucleotides (29). Phosphorothioate content clearly influenced uptake of the parent ASOs, whereas uptake of the ASO conjugates was relatively insensitive to backbone chemistry. Thus, GalNAc conjugation increased uptake of the mixed backbone ASO more than it increased uptake of the full PS ASO, which was largely attributable to the differences in uptake of the respective ASO parents (Figure 5A). This pattern was reflected in activity assays where the parental full PS 5–10–5 MOE displayed a significantly higher potency compared to the mixed backbone ASO, while the corresponding GalNAc conjugates produced similar absolute potencies (Figure 5B). As a result, the relative potency gains were higher with the mixed backbone conjugate than the full PS conjugate, paralleling the results from the uptake experiments.

Uptake of GalNAc–ASOs in ASGR1 inducible HEK cells

While conducting the assays described above it became apparent that the IC50 of the parental full PS 5–10–5 MOE was significantly lower in the ASGR1 expressing HEK cells than we typically see in wild type HEK (Supplementary Figure S2), raising the possibility there is some interaction of the unconjugated ASO with ASGR. To eliminate the possibility that this was an artefact arising from clonal isolation we created an ASGR1 inducible cell line, TREX-ASGR1 (Figure 6). In the absence of doxycycline, uptake of the par-

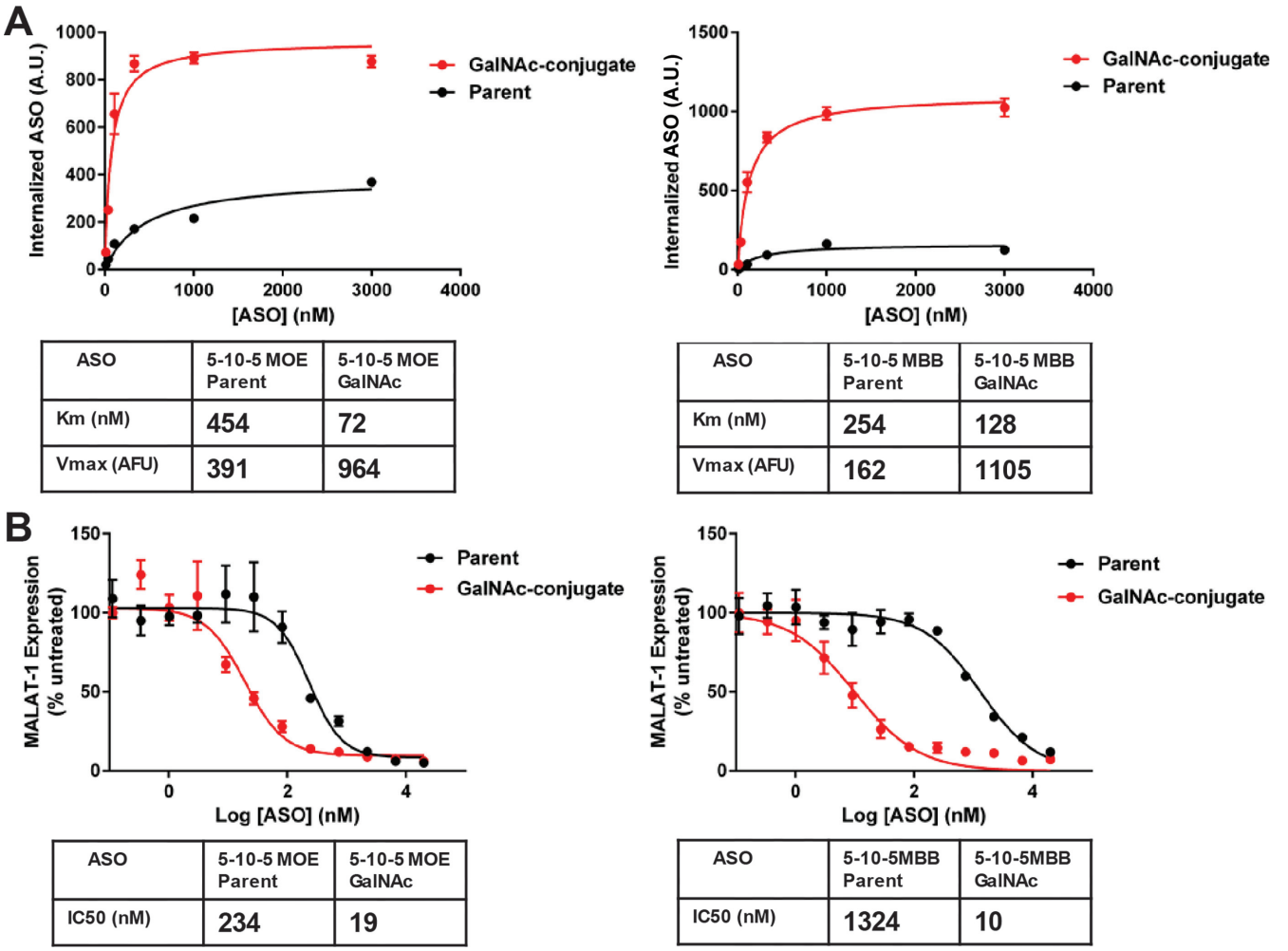

ASO	5-10-5 MOE Parent	5-10-5 MOE GalNAc
Km (nM)	454	72
Vmax (AFU)	391	964

ASO	5-10-5 MBB Parent	5-10-5 MBB GalNAc
Km (nM)	254	128
Vmax (AFU)	162	1105

ASO	5-10-5 MOE Parent	5-10-5 MOE GalNAc
IC50 (nM)	234	19

ASO	5-10-5MBB Parent	5-10-5MBB GalNAc
IC50 (nM)	1324	10

Figure 5. ASGR-mediated uptake of GalNAc–ASO conjugates supersedes effect of ASO phosphorothioate content. (**A**) Uptake of parent and GalNAc conjugates of ASOs representing different phosphorothioate content in ASGR1-expressing HEK line 1A4. Full PS ASOs correspond to ASO 730436, 836716 and mixed backbone ASOs correspond to 890268, 890269 shown in Supplementary Table S1. (**B**) Activity of parent and GalNAc-conjugated ASOs representing different phosphorothioate content in ASGR1-expressing HEK line 1A4. Full PS ASOs correspond to 395251, 890273 and mixed backbone ASOs correspond to 890266, 890267 shown in Supplementary Table S1.

ent and GalNAc-conjugate ASOs were very similar. Following 24 h in the presence of doxycycline, however, there was 2–3-fold increased uptake of the GalNAc ASO conjugate, similar to results previously shown for the non-inducible stable cell line (Figure 6A).

Interestingly, ASGR1 induction also produced a small but consistent increase in uptake of the unconjugated parent (Figure 6A), suggesting ASGR1 may promote uptake of phosphorothioate containing ASOs (23). When TREX ASGR1 cells were tested in activity assays in the absence of doxycycline induction, the ASO parent and ASO conjugate yielded IC50's of approximately one and two micromolar, respectively. Once again, these values are quite similar to untransfected HEK 293 cells. As expected, ASGR1 induction produced a dramatic decrease in the IC50 of the GalNAc-conjugated ASO that was >100-fold lower than in the non-induced cells (Figure 6B). Importantly, there was a clear 2–3-fold decrease in the IC50 of the parent ASO under ASGR induction, supporting our hypothesis that ASGR is able to promote uptake and activity of the parent ASO.

ASGR1 is able to mediate uptake of unconjugated phosphorothioate ASO *in vivo*

Although striking, we suspected the results with the parental ASO might be due to supraphysiologic receptor expression in our *in vitro* cell system. We therefore sought to address this concern by examining the effect of ASGR reduction *in vivo*. In an experiment similar to that presented in Figure 4B, mice were pretreated with an ASO targeting ASGR1 followed by treatment with an unconjugated ASO targeting Factor XI. In agreement with our *in vitro* results, a near complete (>98%) reduction of liver ASGR1 resulted in a ∼2-fold loss of ASO activity (Figure 7). We therefore conclude that ASGR can mediate a small but functionally significant role in uptake and activity of unconjugated phosphorothioate ASOs *in vitro* and *in vivo*.

Relationship between ASGR1 expression and activity of GalNAc ASOs

An important question confronting efforts to identify re-

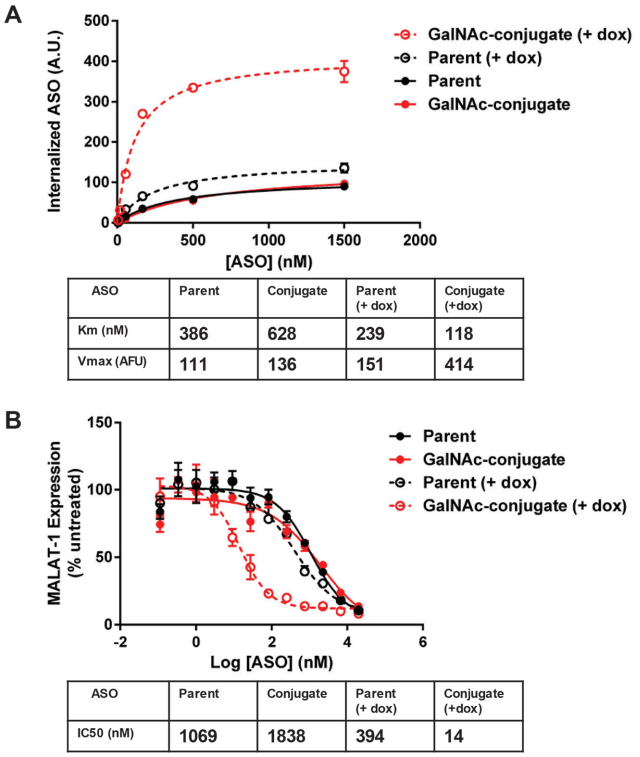

ASO	Parent	Conjugate	Parent (+ dox)	Conjugate (+dox)
Km (nM)	386	628	239	118
Vmax (AFU)	111	136	151	414

ASO	Parent	Conjugate	Parent (+ dox)	Conjugate (+dox)
IC50 (nM)	1069	1838	394	14

Figure 6. Inducible ASGR1 expression demonstrates ASGR1 contributes to uptake and activity of parent phosphorothioate ASOs *in vitro*. (**A**) Uptake of parent and GalNAc-conjugated ASO with and without induction of ASGR1 expression. (**B**) Activity of parent and GalNAc-conjugated ASO with and without induction of ASGR1 expression.

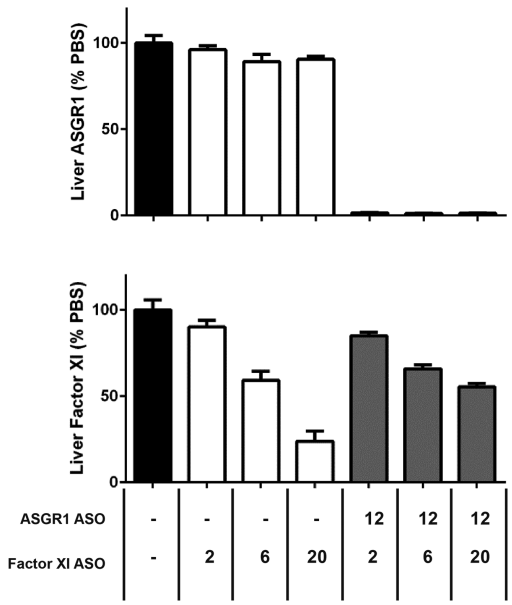

Figure 7. ASGR1 contributes to activity of parent phosphorothioate ASOs *in vivo.* Activity of phosphorothioate ASO dosed alone or in combination with ASO targeting ASGR1 in mouse liver. Doses are expressed as mg ASO/kg body weight.

ceptors capable of mediating productive ASO uptake concerns the role of receptor capacity. Hepatocytes are estimated to express 0.5 – 1 million ASGRs/cell, a level far in excess of most receptors, particularly those involved in cellular signaling (30,31). We sought to determine the relationship between receptor capacity and ASO activity using HEK cell lines representing a range of ASGR expression. Using the GalNAc-conjugated phosphodiester ASO we determined the maximal uptake and Km of several non-inducible ASGR1 expressing cell lines and the inducible TREX-ASGR1 cell line under different levels of ASGR1 induction. We observed a greater than 10 fold range of ASO uptake under these conditions but similar Km values, as would be expected from a Michaelis-Menten model of ligand endocytosis (Figure 8A, top panel). The cell lines were tested in parallel in activity assays and yielded indistinguishable IC50 values over a 3-fold range of ASGR-mediated uptake, with losses in potency appearing under low doxycycline titrations in the TREX-ASGR1 cells (Figure 8A, bottom pane). When the cellular distributions of ASO uptake were examined in the flow cytometry assays, however, it became obvious that the lower levels of induction (0.5 ng/ml and below, data not shown) produced mixed populations consisting of uninduced and maximally induced TREX-ASGR1 cells. It is not possible, therefore, to draw any firm conclusions regarding the reduced potency in TREX-ASGR1 cells under low doxycycline concentrations. Nevertheless, it is clear that ASGR-mediated uptake over at least a three-fold range produced similar sensitivities to GalNAc ASO conjugates, suggesting excess receptor capacity. In addition to the role of receptor capacity, another question of interest is whether the ASGR intrinsically mediates more productive uptake than receptors driving uptake of unconjugated phosphorothioate ASOs. Interpolated values from our uptake experiments, however, suggest that similar amounts of parent and conjugated ASO are internalized at their respective IC50 concentrations (Supplementary Figure S4). According to the available data, therefore, ASGR-mediated potency results from increased uptake at low ASO concentrations rather than diverting ASO to a more productive internalization pathway. To examine the role of receptor capacity *in vivo,* mice received increasing doses of the unconjugated ASO targeting ASGR1 simultaneously with three different doses of the Factor XI GalNAc–ASO conjugate. Remarkably, a knockdown of ASGR1 by as much as 78% produced little discernable effect on the activity of the Factor XI GalNAc-conjugate (Figure 8B). Only in mice with >98% knockdown of ASGR1 was activity of the Factor XI GalNAc-conjugate lost. These results show that there is an excess capacity of ASGR-mediated uptake of GalNAc ASO conjugates in mouse liver *in vivo* and suggest that far lower ASGR expression levels are capable of fully conferring the potency gains seen with GalNAc–ASO conjugates.

DISCUSSION

The use of antisense oligonucleotides to modify mRNA levels or pre-mRNA splicing is a proven approach with demonstrated therapeutic benefit and tremendous potential to treat previously intractable human diseases. The pri-

A

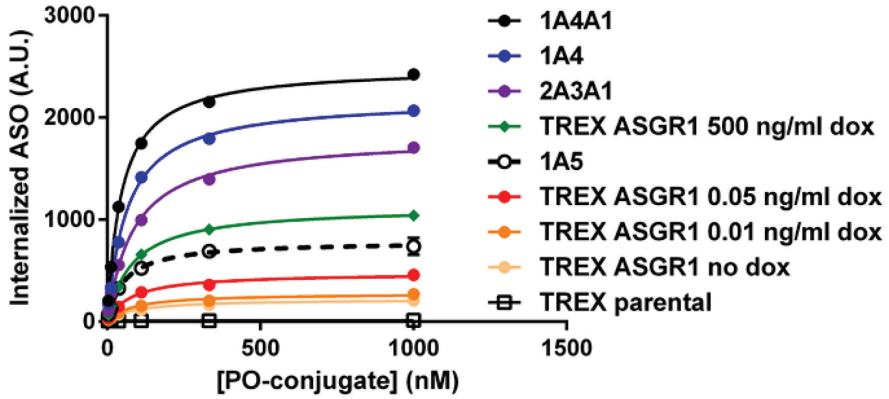

ASO	TREX Parental	TREX-ASGR1 no dox	TREX-ASGR1 0.01 ng/m dox	TREX-ASGR1 0.05 ng/m dox	1A5	TREX-ASGR1 500 ng/m dox	2A3A1	1A4	1A4A1
Km (nM)	n/a	86	80	78	54	80	86	64	46
Vmax	n/a	219	277	419	788	1125	1812	2182	2494

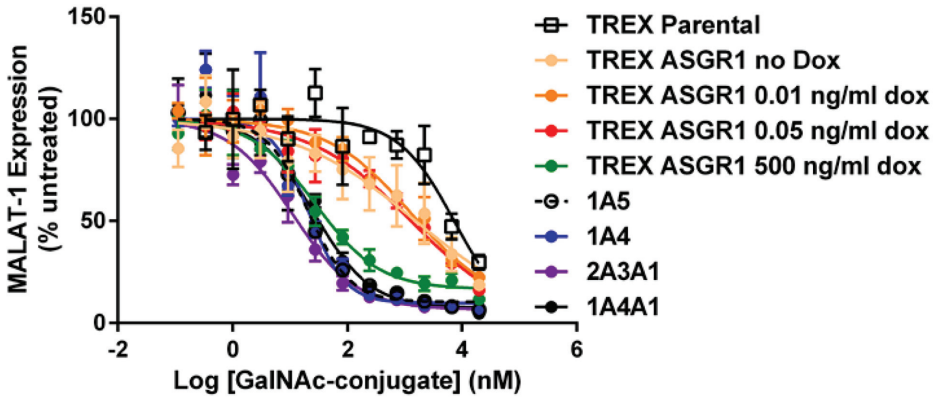

Cell Line	TREX Parental	TREX-ASGR1 no dox	TREX-ASGR1 0.01 ng/ml dox	TREX-ASGR1 0.05 ng/ml dox	1A5	TREX-ASGR1 500 ng/ml dox	2A3A1	1A4	1A4A1
IC50 (nM)	4957	658	920	599	20	23	15	19	25

B

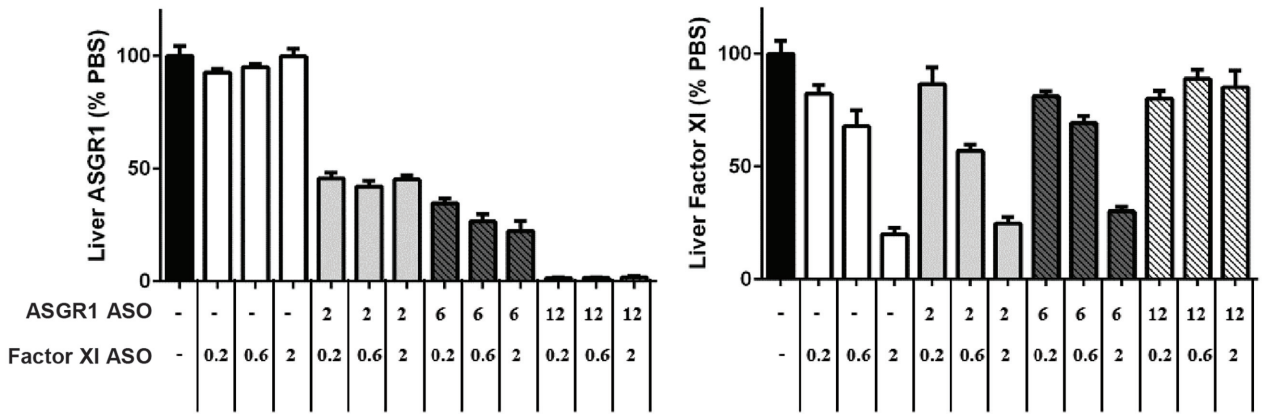

Figure 8. There is a large excess capacity of ASGR1 in both engineered HEK cells and *in vivo*. (**A**) Comparison of uptake and activity of GalNAc-conjugated ASO in HEK 293 cell clones representing different levels of ASGR1 expression. (**B**) Activity of GalNAc-conjugated ASO in mouse liver under different levels of ASGR1 knockdown. Doses are expressed as mg ASO/kg body weight.

mary challenge to their wider application, however, is insufficient cellular uptake and limited potency in a number of tissues and cell types. The conjugation of ASOs to receptor ligands has emerged as an effective strategy to address this barrier. GalNAc-conjugation not only increases the potency of ASOs targeting transcripts expressed in liver tissue but also dramatically shifts liver ASO uptake from non-parenchymal cells to hepatocytes (9), thereby promoting more efficient targeting towards the cell type of interest.

In addition to enhancing potency, the ASGR/GalNAc interaction, represents an excellent model system with which to probe essential questions regarding the requirements for effective receptor-mediated ASO uptake into cells. In the present study we compared ASO internalization and knockdown activity in pre-existing hepatic cell models representing different ASGR expression levels and discovered an apparent disconnect between GalNAc-mediated ASO uptake and resulting knockdown activity. We believe this is primarily due to the intrinsic recalcitrance of HepG2 cells in free uptake assays, underscoring the limitations of available immortal cell lines endogenously expressing the ASGR. Exogenous expression in HEK 293 cells is an attractive *in vitro* model to overcome such limitations but carries with it the concern that high level heterologous expression may produce artefactual phenotypes unrelated to the *in vivo* behavior of native tissue. In contrast to this well-founded concern, we found that ASGR-expressing HEK cells mirrored the *in vivo* behavior of hepatocytes to a remarkable degree. Not only did the engineered cells internalize and respond to GalNAc–ASO conjugates in manners similar to isolated hepatocytes, they revealed unanticipated properties of *in vivo* ASGR-mediated ASO uptake. Examples include the dispensability of ASGR2 in productive conjugate uptake, the influence of ASGR1 in uptake of phosphorothioate ASOs, and the significant excess capacity of ASGR for active conjugate uptake. For these reasons, we believe engineered cells, though artificial, are an effective tool in the pursuit of potential receptor/ligand pairs for targeted ASO delivery, particularly for cell types and tissues that are underrepresented in available immortal cell lines.

Moving forward, there are several implications of the current work that can inform the search for additional receptors capable of effective ASO delivery. ASGR-mediated uptake is particularly well suited to a K_m model as the ASGR quickly releases cargo in the acidifying endosome and is efficiently recycled thereafter, resulting in catalytic uptake whereby one receptor may internalize multiple rounds of cargo. We observed a low K_m of ASO uptake in all ASGR models showing enhanced activity to GalNAc conjugates. All things being equal, a low K_m is assumed to be beneficial for ASO uptake because maximal uptake occurs at low ASO concentrations. We expect there to be an interdependent relationship between receptor number and K_m, where low receptor expression requires a low K_m for saturated uptake but a highly expressed receptor with a high K_m may mediate active uptake at partial saturation.

The ASGR is both highly expressed and has a low K_m for GalNAc conjugates, assuring high uptake at low ASO concentrations. Moreover, efficient release of cargo within the acidifying endosome is assumed to be important for both endosomal release and recycling of an unoccupied receptor. The GalNAc-ASGR interaction is pH sensitive, allowing efficient dissociation in acidifying endosomes. When we tested the activity of GalNAc conjugates over a range of ASGR expression, it was clear that there was excess receptor capacity both *in vivo* and *in vitro*. This supports the consideration of other receptor systems lacking the extremely high expression of ASGR measured in hepatocytes, provided such receptors are internalizing high-affinity conjugates and efficiently separating from them within the endosomal system.

Previous efforts to accomplish targeted delivery of biomolecules have met with limited success, although detailed analyses of concentration-dependent cargo uptake have largely been lacking. We believe our results demonstrate the importance of detailed comparisons of cargo flux with respect to concentration and time. Nevertheless, it must be acknowledged that there are many potential barriers to receptor-mediated tissue-targeted delivery irrespective of a given receptor's capacity to internalize cargo. Different cell types clearly have different intrinsic sensitivities to ASO-mediated knock-down, as evidenced by the profound insensitivity of HepG2 cells to GalNAc–ASO conjugates despite considerably increased uptake. It is possible some tissues or associated cell populations are similarly insensitive *in vivo,* resulting in an inability to target that tissue regardless of the amount of ASO internalized (32). Similarly, as the exact sorting steps and endosomal dynamics necessary for ASO activity remain unclear, it seems likely that some receptors may fail to internalize ASO productively as a result of their specific membrane trafficking properties. Despite these concerns, we remain optimistic that the ASGR is not sui generis and additional receptors will prove to be effective mediators of tissue-targeted delivery.

Based upon our knowledge of the ASGR what properties might these other receptors share? The ASGR is a long studied receptor that traverses the well characterized clathrin-dependent internalization pathway shared by the majority of nutrient and signaling receptors. It therefore seems likely that productive free uptake occurs, or can occur, through the prosaic clathrin-dependent pathway rather than exotic endocytic mechanisms yet to be defined. In addition, we found no evidence that the ASGR-mediated uptake is intrinsically more productive than default phosphorothioate-mediated uptake. This implies that the productive endocytic pathway is the rule rather than the exception and, combined with data suggesting moderate receptor expression can support productive free uptake, suggests other receptor-ligand pairs can mediate functional ASO uptake and tissue-targeted delivery.

SUPPLEMENTARY DATA

Supplementary Data are available at NAR Online.

FUNDING

Funding for open access charge: Ionis Pharmaceuticals, Inc.
Conflict of interest statement. None declared.

REFERENCES

1. Beltinger,C., Saragovi,H.U., Smith,R.M., LeSauteur,L., Shah,N., DeDioniso,L., Christensen,L., Raible,A., Jartt,L. and Gewirtz,A.M. (1995) Binding, uptake, and intracellular trafficking of phosphorothioate-modified oligodeoxynucleotides. *J. Clin. Invest.*, **95**, 1814–1823.
2. Geary,R.S., Norris,D., Yu,R. and Bennett,C.F. (2015) Pharmacokinetics, biodistribution and cell uptake of antisense oligonucleotides. *Adv. Drug Deliv. Rev.*, **87**, 46–51.
3. Miller,C.M., Donner,A.J., Blank,E.E., Egger,A.W., Kellar,B.M., Østergaard,M.E., Seth,P.P. and Harris,E.N. (2016) Stabilin-1 and Stabilin-2 are specific receptors for the cellular internalization of phosphorothioate-modified antisense oligonucleotides (ASOs) in the liver. *Nucleic Acids Res.*, **44**, 2782–2794.
4. Varkouhi,A.K., Scholte,M., Storm,G. and Haisma,H.J. (2011) Endosomal escape pathways for delivery of biologicals. *J. Control. Release*, **151**, 220–228.
5. Wittrup,A., Ai,A., Liu,X., Hamar,P., Trifonova,R., Charisse,K., Manoharan,M., Kirchhausen,T. and Lieberman,J. (2015) Visualizing lipid-formulated siRNA release from endosomes and target gene knockdown. *Nat. Biotechnol.*, **33**, 870–876.
6. Koller,E., Vincent,T.M., Chappell,A., De,S., Manoharan,M. and Bennett,C.F. (2011) Mechanisms of single-stranded phosphorothioate modified antisense oligonucleotide accumulation in hepatocytes. *Nucleic Acids Res.*, **39**, 4795–4807.
7. Juliano,R.L. (2016) The delivery of therapeutic oligonucleotides. *Nucleic Acids Res.*, **44**, 6518–6548.
8. Biessen,E.A., Vietsch,H., Rump,E.T., Fluiter,K., Kuiper,J., Bijsterbosch,M.K. and van Berkel,T.J. (1999) Targeted delivery of oligodeoxynucleotides to parenchymal liver cells in vivo. *Biochem. J.*, **340**, 783–792.
9. Prakash,T.P., Graham,M.J., Yu,J., Carty,R., Low,A., Chappell,A., Schmidt,K., Zhao,C., Aghajan,M., Murray,H.F. *et al.* (2014) Targeted delivery of antisense oligonucleotides to hepatocytes using triantennary N-acetyl galactosamine improves potency 10-fold in mice. *Nucleic Acids Res.*, **42**, 8796–8807.
10. Nair,J.K., Willoughby,J.L., Chan,A., Charisse,K., Alam,M.R., Wang,Q., Hoekstra,M., Kandasamy,P., Kel'in,A.V., Milstein,S. *et al.* (2014) Multivalent N-acetylgalactosamine-conjugated siRNA localizes in hepatocytes and elicits robust RNAi-mediated gene silencing. *J. Am. Chem. Soc.*, **136**, 16958–16961.
11. Hudgin,R.L., Pricer,W.E., Ashwell,G., Stockert,R.J. and Morell,A.G. (1974) The isolation and properties of a rabbit liver binding protein specific for asialoglycoproteins. *J. Biol. Chem.*, **249**, 5536–5543.
12. Grewal,P.K. (2010) The Ashwell-Morell receptor. *Methods Enzymol.*, **479**, 223–241.
13. Baenziger,J.U. and Maynard,Y. (1980) Human hepatic lectin. Physiochemical properties and specificity. *J. Biol. Chem.*, **255**, 4607–4613.
14. Graham,M.J., Crooke,S.T., Monteith,D.K., Cooper,S.R., Lemonidis,K.M., Stecker,K.K., Martin,M.J. and Crooke,R.M.J. (1998) In vivo distribution and metabolism of a phosphorothioate oligonucleotide within rat liver after intravenous administration. *Pharmacol. Exp. Ther.*, **286**, 447–458.
15. Graham,M.J., Crooke,S.T., Lemonidis,K.M., Gaus,H.J., Templin,M.V. and Crooke,R.M. (2001) Hepatic distribution of a phosphorothioate oligodeoxynucleotide within rodents following intravenous administration. *Biochem. Pharmacol.*, **62**, 297–306.
16. Liu,W., Hou,Y., Chen,H., Wei,H., Lin,W., Li,J., Zhang,M., He,F. and Jiang,Y. (2011) Sample preparation method for isolation of single-cell types from mouse liver for proteomic studies. *Proteomics*, **11**, 3556–3564.
17. Steirer,L.M., Park,E.I., Townsend,R.R. and Baenziger,J.U. (2009) The asialoglycoprotein receptor regulates levels of plasma glycoproteins terminating with sialic acid α2,6-galactose. *J. Biol. Chem.*, **284**, 3777–3783.
18. Lee,R.T., Lin,P. and Lee,Y.C. (1984) New synthetic cluster ligands for galactose/N-acetylgalactosamine-specific lectin of mammalian liver. *Biochemistry.*, **23**, 4255–4261.
19. Zhao,Q., Matson,S., Herrera,C.J., Fisher,E., Yu,H. and Krieg,A.M. (1993) Comparison of cellular binding and uptake of antisense phosphodiester, phosphorothioate, and mixed phosphorothioate and methylphosphonate oligonucleotides. *Antisense Res. Dev.*, **3**, 53–66.
20. Teplova,M., Minasov,G., Tereshko,V., Inamati,G.P., Cook,P.G., Manoharan,M. and Egli,M. (1999) Crystal structure and improved antisense properties of 2′-O-(2-methoxyethyl)-RNA. *Nat. Struct. Biol.*, **6**, 535–539.
21. Li,Y., Huang,G., Diakur,J. and Wiebe,L.I. (2008) Targeted delivery of macromolecular drugs: asialoglycoprotein receptor (ASGPR) expression by selected hepatoma cell lines used in antiviral drug development. *Curr. Drug Deliv.*, **5**, 299–302.
22. Severgnini,M., Sherman,J., Sehgal,A., Jayaprakash,N.K., Aubin,J., Wang,G., Zhang,L., Peng,C.G., Yucius,K., Butler,J. *et al.* (2012) A rapid two-step method for isolation of functional primary mouse hepatocytes: cell characterization and asialoglycoprotein receptor based assay development. *Cytotechnology*, **64**, 187–195.
23. Schmidt,K., Prakash,T.P., Donner,A.J., Kinberger,G.A., Gaus,H.J., Low,A., Østergaard,M.E., Bell,M., Swayze,E.E. and Seth,P.P. (2017) Characterizing the effect of GalNAc and phosphorothioate backbone on binding of antisense oligonucleotides to the asialoglycoprotein receptor. *Nucleic Acids Res.*, **45**, 2294–2306.
24. Bischoff,J., Libresco,S., Shia,M.A. and Lodish,H.F. (1988) The H1 and H2 polypeptides associate to form the asialoglycoprotein receptor in human hepatoma cells. *J. Cell Biol.*, **106**, 1067–1074.
25. Shia,M.A. and Lodish,H.F. (1989) The two subunits of the human asialoglycoprotein receptor have different fates when expressed alone in fibroblasts. *Proc. Natl. Acad. Sci. U.S.A.*, **86**, 1158–1162.
26. Shenkman,M., Ayalon,M. and Lederkremer,G.Z. (1997) Endoplasmic reticulum quality control of asialoglycoprotein receptor H2a involves a determinant for retention and not retrieval. *Proc. Natl. Acad. Sci. U.S.A.*, **14**, 11363–11368.
27. Ishibashi,S., Hammer,R.E. and Herz,J. (1994) Asialoglycoprotein receptor deficiency in mice lacking the minor receptor subunit. *J. Biol. Chem.*, **269**, 27803–27806.
28. Grewal,P.K., Uchiyama,S., Ditto,D., Varki,N., Le,D.T., Nizet,V. and Marth,J.D. (2008) The Ashwell receptor mitigates the lethal coagulopathy of sepsis. *Nat. Med.*, **14**, 648–655.
29. Prakash,T.P., Yu,J., Migawa,M.T., Kinberger,G.A., Wan,W.B., Ostergaard,M.E., Carty,R.K., Vasquez,G., Low,A., Chappell,A. *et al.* (2016) Comprehensive structure-activity relationship of triantennary N-acetylgalactosamine conjugated antisense oligonucleotides for targeted delivery to hepatocytes. *J. Med. Chem.*, **59**, 2718–2733.
30. Spiess,M. (1990) The asialoglycoprotein receptor: a model for endocytic transport receptors. *Biochemistry*, **29**, 10009–10018.
31. Stockert,R.J. (1995) The asialoglycoprotein receptor: relationships between structure, function, and expression. *Physiol. Rev.*, **75**, 591–609.
32. Donner,A.J., Wancewicz,E.V., Murray,H.M., Greenlee,S., Post,N., Bell,M., Lima,W.F., Swayze,E.E. and Seth,P.P. (2017) Co-Administration of an Excipient Oligonucleotide Helps Delineate Pathways of Productive and Nonproductive Uptake of Phosphorothioate Antisense Oligonucleotides in the Liver. *Nucleic Acid Ther.*, **27**, 209–220.